

Observation of Resonant Tunneling between Macroscopically Distinct Quantum Levels

R. Rouse, Siyuan Han, and J. E. Lukens

Department of Physics, University at Stony Brook, Stony Brook, New York 11794

(Received 20 April 1995)

We report the first observation of resonant tunneling of a system between two macroscopically distinct states: energy levels in different fluxoid wells of a weakly damped superconducting quantum interference device which differ in mean current by approximately $6 \mu\text{A}$. Near 50 mK, the tunneling rate $\Gamma(\Phi_x)$ from the metastable well vs applied flux Φ_x is found to exhibit a series of local maxima where the levels (spaced by ≈ 1.9 K) in the two wells cross. The positions of these maxima agree well with the level crossings calculated using independently determined system parameters.

PACS numbers: 74.50.+r, 03.65.-w, 73.40.Gk

Throughout the history of quantum mechanics, there have been a series of paradoxes resulting from attempts to reconcile the description of nature at the microscopic level with everyday observations of macroscopic objects. While many explanations have been proposed, the dilemma remains in the minds of many [1,2]. It is of some interest then to try to observe quantum effects, familiar in the microscopic world, in variables describing macroscopically distinct states. Josephson junctions, along with the superconducting quantum interference device (SQUID), have proven to be excellent systems for such investigations. The flux Φ linking the SQUID (or the phase difference across a current biased junction) describes the collective motion of a macroscopic number of particles and yet manifests quantum behavior at accessible temperatures. Further, it is possible to characterize these systems very well, permitting quantitative comparison with theory. Tunneling of these macroscopic variables to the continuum (MQT) [3–7] has been widely studied and generally found to be in excellent agreement with theory. Level quantization within a well has been observed [8], again agreeing with theory [9,10]. However, answers to more fundamental questions (including macroscopic quantum coherence [1]) require measurements of the behavior of systems involving transitions between macroscopically distinct, discrete final and initial states. Extensive theoretical analysis of such transitions has been done using the two state approximation to the SQUID [11,12]. These predict that, under conditions of low damping and temperature, Φ should display the quantum interference behavior familiar for microscopic systems. The limited experimental work on such systems has tended to confirm these predictions in the higher damping regime where evidence for discrete final states is indirect [13]. Recently reported results on magnetic systems have been interpreted in terms of macroscopic quantum behavior [14]. However, there is currently substantial controversy as to the interpretation of the results that, it is argued, differ markedly from theory [15]. In this Letter, we report the observation of resonances in the tunneling rate of the flux between two macroscopically distinct fluxoid wells of a SQUID when

the ground state of the upper well is aligned with an excited state in the lower well. We refer to this phenomenon, in which the quantized final and initial states differ in mean current by about $6 \mu\text{A}$, as macroscopic resonant tunneling (MRT). A number of authors have predicted a related phenomenon in current biased junctions [16,17]. There the problem is somewhat different since the system must, in general, finally escape to the continuum, or finite voltage state, to allow observation of the effect.

The sample [shown schematically in Fig. 1(a)] consists of a large superconducting loop (the rf SQUID) of inductance L which is interrupted by a small loop (the dc SQUID) containing two Josephson junctions. For our sample parameters (see below), the dc SQUID is well approximated by a single junction with a critical current $I_c(\Phi_{x\text{dc}})$ which can be modulated by an applied flux $\Phi_{x\text{dc}}$ [18]. Additional coils apply an independent flux Φ_x to the rf SQUID and couple the rf SQUID to a magnetometer which monitors the flux Φ linking it. The classical equation of motion for Φ is homologous to that of a particle of mass C , the junction capacitance, moving with damping R^{-1} in a potential $U(\Phi, \Phi_x)$. Here, R is an equivalent shunt resistance across the junction which represents the damping of the system. The potential U is given by

$$U(\Phi, \Phi_x) = U_0 \left[\frac{1}{2}(\varphi - \varphi_x)^2 + \beta_L \cos(\varphi) \right], \quad (1)$$

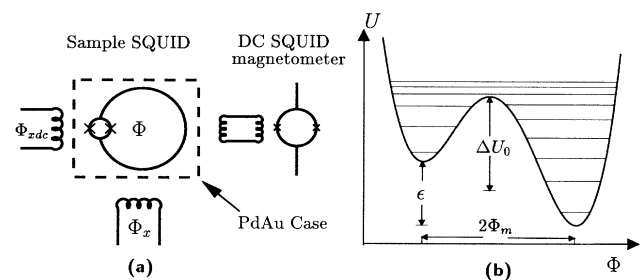


FIG. 1. (a) Schematic of experimental setup. (b) Asymmetrical SQUID potential ($\Phi_x > \Phi_0/2$) with quantized energy levels.

where φ_x and φ are fluxes in units of $\Phi_0/2\pi$ measured with respect to $\Phi_0/2$, $U_0 \equiv \Phi_0^2/4\pi^2L$, and $\beta_L \equiv 2\pi LI_c(\Phi_{x\text{dc}})/\Phi_0$ is a measure of the total critical current in terms of the current required to create Φ_0 in the loop. For $\varphi_x = 0$, this potential is a symmetric double well with the left and right wells corresponding to the 0 and 1 fluxoid states of the SQUID, respectively. For large enough R , i.e., high $Q \equiv RC\omega_0$ (where ω_0 is the small oscillation frequency), the energy levels in these wells are sharply quantized with a fractional width of approximately Q^{-1} [19,20]. For $\varphi_x \neq 0$, the potential is tilted, as shown in Fig. 1(b), resulting in an energy difference $\epsilon = 2U_0\varphi_m\varphi_x$ between the minima of the wells, where $\pm\varphi_m(\beta_L)$ are the locations of the minima of the potential for $\varphi_x = 0$. We label the levels of the upper (lower) well by n_u (n_l) with $n_i = 0, 1, \dots$. As noted above, I_c can be modulated using $\Phi_{x\text{dc}}$, allowing $\beta_L = \beta_{L0} \cos(\pi\Phi_{x\text{dc}}/\Phi_0)$, and thus the shape of the potential, to be varied *in situ*. The energy barrier ΔU_0 between the wells for $\epsilon = 0$ is a function of β_L and can therefore also be varied *in situ*. As φ_x is increased the barrier ΔU for escape from the upper well decreases roughly linearly with ϵ , giving $\Delta U(\Phi_x, \Phi_{x\text{dc}}) \approx \Delta U_0(\Phi_{x\text{dc}}) - \epsilon(\Phi_x)/2$.

The sample SQUID was fabricated, along with pickup loops for Φ_x and $\Phi_{x\text{dc}}$, on an oxidized Si substrate using Nb/ AlO_x /Nb junctions. The junctions, which were patterned using electron beam lithography, had a programmed area of $1 \mu\text{m}^2$ each and a specific capacitance of $40 \text{ fF}/\mu\text{m}^2$, giving a nominal total capacitance $C_\Sigma = 80 \text{ fF} \pm 30\%$. The typical subgap resistance for such junctions fabricated in our laboratory is greater than $10^5 \Omega$ at low temperature. The rf SQUID—a square $140 \mu\text{m}$ on a side—along with the pickup loops were patterned in a gradiometer geometry to improve the isolation of the sample. The Si chip was wrapped in AuPd foil, which has a sheet resistance of 0.18Ω and a thickness of $1.6 \mu\text{m}$ and was separated from the plane of the sample by $125 \mu\text{m}$. This foil had a cutoff at about 1 GHz and helped to shield the sample from any high frequency noise which bypassed the low temperature filters on the field coils as well as from the Josephson oscillation of the magnetometer, which was a dc SQUID operating near 100 GHz. This foil was also the dominant source of damping for the sample, being equivalent to a shunt resistance of about 3–6 k Ω across the junction at frequencies below 1 GHz. The coupling of the sample to the magnetometer and the two bias fluxes was through coils in a plane normal to the chip outside the foil. The coils were shielded from each other using superconducting shielding to minimize cross talk. The mutual inductances of the sample SQUID to the field coils and the magnetometer were less than 2 pH, giving a negligible damping by the coils. This entire assembly was enclosed in a Nb shield inside a copper cell filled with ^4He . This cell was located on a temperature regulated platform coupled to the mixing chamber of a dilution refrigerator. All data reported here

were obtained at a platform temperature of about 50 mK. The ambient field was reduced to 10^{-5} G using Mumetal shielding. This setup gave a very high degree of field stability, e.g., for an applied flux Φ_x to the rf SQUID of zero, the actual flux through the SQUID changed by less than $10^{-4}\Phi_0$ over a period of a month while the experiment was being run. Using measurements at high temperatures where the transitions between the wells are thermally activated, it is possible to accurately determine the sample parameters entering the potential [18]. Such measurements give $L = 210 \text{ pH} \pm 5\%$ and $\beta_{L0} = 2.00 \pm 5\%$ as well as showing that the critical currents of the two junctions comprising the dc SQUID [which has a loop inductance of $(8 \pm 1) \text{ pH}$] are equal within 1%. Thus the 1D potential [Eq. (1)] is an excellent approximation to the true 2D potential for the system [18]. These parameters, together with the values of C_Σ and R quoted above, give $\omega_0 \approx 40 \text{ GHz}$ (1.9 K) and $Q \geq 50$ for a barrier height $\Delta U \approx 7 \text{ K}$ where MRT transitions become observable. The parameter $\alpha \equiv (\varphi_m/\pi)^2 R_Q/R$ [$R_Q \equiv h/(2e)^2 \approx 6.5 \text{ k}\Omega$], which characterizes the damping for the two level SQUID [11], would then be less than the critical value of 0.5 since $\varphi_m = 1.4$.

The experiment consists of varying Φ_x linearly in time to tilt the potential at a rate of about 20 K/s, reducing the barrier of the upper well until a fluxoid transition occurs. The value of Φ_x for this transition is then recorded and the sign of $d\Phi_x/dt$ reversed, tilting the potential back until the system returns to the original well. This process is repeated approximately 10^4 times, generating a histogram of the transition probability $P(\epsilon)$. Figure 2(a) shows one such histogram obtained for $\Delta U_0 = 16.3 \text{ K}$. As one can see, $P(\epsilon)$ has a series of maxima separated by about 1.9 K. The arrows indicate the location of the calculated crossings of levels n_l in the lower well with the $n_u = 0$ level of the upper well. We identify all peaks except the leftmost as due to MRT from $n_u = 0$ to $n_l \approx \epsilon/\hbar\omega_0$. We identify the leftmost peak, labeled PAT, as a photon assisted tunneling peak in which the system is first pumped to $n_u = 3$ by the residual 100 GHz flux from the SQUID magnetometer and then tunnels to $n_l \approx \epsilon/\hbar\omega_0 + 3$. This is discussed in more detail below.

In general $P(\epsilon) = \Gamma(\epsilon)[1 - \int_0^\epsilon P(x) dx](d\epsilon/dt)^{-1}$, where the factor in the square brackets is just the probability that the system has not yet undergone a transition and $\Gamma(\epsilon)$ is the total escape rate from the upper well. This can be inverted to obtain $\Gamma(\epsilon)$, which is shown in Fig. 2(b). For contrast, the dashed lines in Figs. 2(a) and 2(b) show the predicted transition probability and rate calculated using the WKB approximation for tunneling from the bottom of the upper well into a continuum at zero temperature and zero damping. Since $Q \geq 50$ for our system, damping corrections to $\Gamma_{\text{WKB}}(\epsilon)$ are negligible [3]. Note that the overall trend of $\Gamma(\epsilon)$, aside from the MRT oscillations, is not accurately given by $\Gamma_{\text{WKB}}(\epsilon)$, i.e., the overall rate is higher than expected closer to the

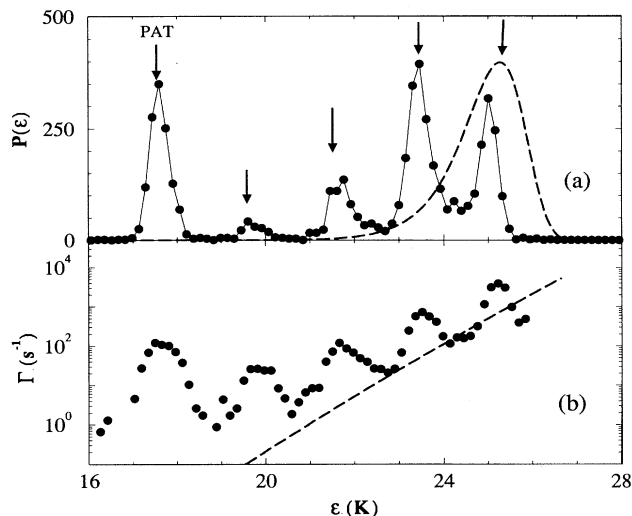


FIG. 2. (a) Measured transition probability $P(\epsilon)$ vs potential tilt for $\Delta U_0 = 16.3$ K (circles). Calculated WKB transition probability for tunneling to a continuum is shown by the dashed line. Arrows indicate calculated level crossings. (b) Circles show transition rates obtained from $P(\epsilon)$ (see text). Calculated WKB rate into a continuum is shown by the dashed line.

PAT peak. This is, of course, expected for the PAT peak itself since these transitions are from the $n_u = 3$ level where the barrier is lower by $\hbar\omega_{\text{rf}} = 4.88$ K than for the MRT transitions at the same ϵ . The excess rate for the lower MRT peaks could be accounted for by residual PAT transitions in the tail of the PAT resonance. However, we have not attempted to correct for this effect since an adequate theory of the PAT line shape does not exist. The widths $\Delta\Gamma(\epsilon)$ of the PAT and MRT resonances at $T = 50$ mK are (within $\pm 50\%$) 0.4 K under all conditions, i.e., for both PAT and MRT peaks, independent of the final state n_l or (for PAT peaks) of the proximity to a level crossing.

The energy levels [Fig. 1(b)] have been calculated in the limit of zero damping and temperature by numerically solving the SQUID Hamiltonian:

$$H_0(\Phi, \Phi_x, \Phi_{x\text{dc}}) = p_\Phi^2/2m + U(\Phi, \Phi_x, \Phi_{x\text{dc}}), \quad (2)$$

where $p_\Phi = -i\hbar\partial/\partial\Phi$ and the “mass” $m = C_\Sigma$. A basis set of 80 harmonic oscillator wave functions with frequency $\omega = (LC_\Sigma)^{-1/2}$ was used for these calculations. The results for $\Delta U_0 = 16.3$ K are presented in Fig. 3 showing the energy levels $E_n^{(l)}$ and $E_n^{(u)}$ of these wells with respect to $E_0^{(l)}$. These appear as diagonal and nearly horizontal solid lines, respectively. Also shown is the barrier energy $\Delta U(\epsilon)$ (thick solid line) and several levels above the barrier. The level crossings, ϵ_{MRT} , between $n_u = 0$ and excited states of the lower well occur where the diagonal lines $E_n^{(l)}$ cross the abscissa (where they are truncated). The expected location of a PAT peak, ϵ_{PAT} ,

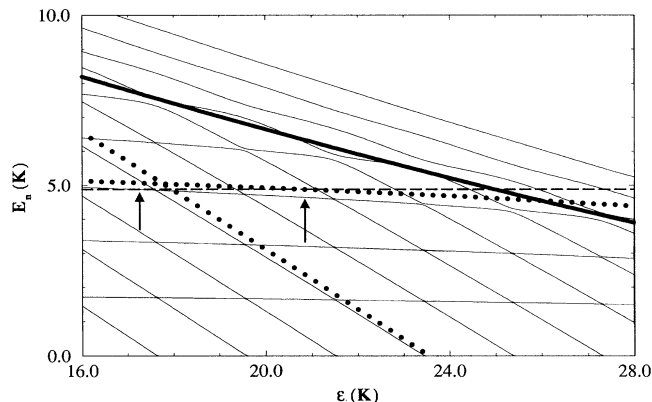


FIG. 3. Solid lines are the calculated energy levels for the upper (horizontal) and lower (diagonal) wells, given with respect to the zero level in the upper well, for $\Delta U_0 = 16.3$ K. The thick solid line is the top of the energy barrier. Dotted lines show two levels for $\Delta U_0 = 17.7$ K. Arrows mark the photon (dashed line) absorption resonances for the two values of ΔU_0 .

is given by the intersection (arrow) of the $n_u = 3$ level and the constant energy line representing $\hbar\omega_{\text{rf}}$ (dashed line) for the magnetometer. The level shifts due to damping have been calculated for similar systems [19,20] and found to be negligible. To illustrate the effects of changes in ΔU_0 on the positions of the resonances, we have also shown the $n_u = 3$ and $n_l = 12$ levels for $\Delta U_0 = 17.7$ K (dotted lines). As one can see, ϵ_{MRT} changes very slowly with ΔU_0 while ϵ_{PAT} varies rapidly. This difference makes the differentiation of the MRT and PAT peaks quite straightforward.

The residual rf flux, Φ_{rf} , from the magnetometer has been neglected in the calculation of the SQUID wave functions. We can obtain a limit on the amplitude of this rf field by comparing the occupation of the $n_u = 3$ level estimated from the amplitude of the PAT peak to that calculated from the pumping rate as a function of the rf level by treating the rf flux as a perturbation, $H_1 = U_0\Phi\Phi_{\text{rf}}\sin(\omega_{\text{rf}}t)$, to H_0 . This calculation implies an rf flux with $\Phi_{\text{rf}} < 4 \times 10^{-5}\Phi_0$ for $Q = 50$. The damping due to the foil will be much less at 100 GHz than at 1 GHz, leading to a $Q \gg 50$. This should therefore serve as an upper limit on the rf flux.

Figure 4 shows the calculated positions ϵ_{MRT} of several of the level crossings as a function of the symmetric barrier height, ΔU_0 , along with the measured locations of the MRT peaks for 34 data sets taken for a range of ΔU_0 . The sample parameters L , β_{L0} , and C have been adjusted for the best fit to the data. These best fit values $L_{\text{fit}} = 210 \pm 2$ pH, $\beta_{L0,\text{fit}} = 1.99 \pm 0.04$, and $C_{\Sigma,\text{fit}} = 82 \pm 4$ fF are in excellent agreement with those determined independently as quoted above. The solid triangles show the measured positions of the PAT peaks.

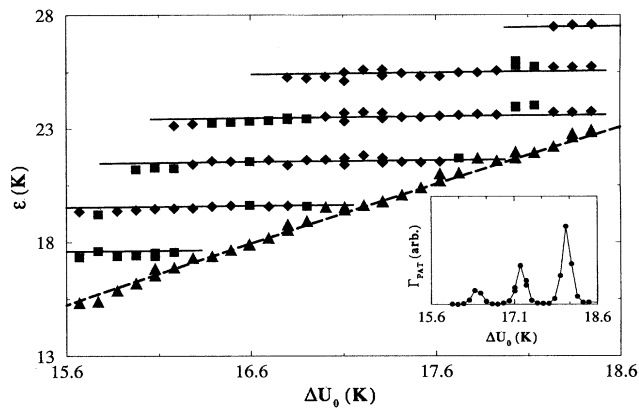


FIG. 4. Measured (diamonds and squares) and calculated (solid lines) positions, in energy bias (ϵ), of MRT peaks vs ΔU_0 . The diamonds show the peak position from fitting $\Gamma(\epsilon)$ to a Gaussian while the squares are the local maxima in $P(\epsilon)$. Triangles are the measured positions of the PAT peaks compared to the calculated position of the photon absorption resonance (dashed line). The inset shows the measured rate at the PAT peaks vs ΔU_0 .

The calculated values of $\epsilon_{\text{PAT}}(\Delta U_0)$, using the same values for the fitting parameters, are indicated by the dashed line, again showing excellent agreement. Since ϵ_{PAT} periodically coincides with a level crossing as ΔU_0 is varied, one would expect a periodic variation in the amplitude of the PAT peak. This is indeed observed as shown in the inset of Fig. 4. We note that if the width of the resonance was determined by the width of the final state one would expect the position of the PAT peaks to be pulled much more strongly to the level crossing positions than is evidenced by the data.

To summarize, we have seen clear evidence for resonant tunneling of the flux between quantized energy levels in different fluxoid states of a SQUID. These states are clearly macroscopically distinct, differing in mean loop current by about $6 \mu\text{A}$. The energy levels of this system have been calculated using the independently measured potential that describes the SQUID and found to agree with the positions of the resonant peaks in the tunneling rates quite accurately. The dependence of the level spacing within a well has also been measured as a function of the tilt and barrier height of the symmetric potential

(which was varied *in situ*) using photon assisted tunneling and found to be well described by the calculated level spacings.

We wish to acknowledge many useful discussions with K. K. Likharev, D. Averin, S. Kivelson, S. Chakravarty, and X. Wen. This work was supported by the Office of Naval Research.

-
- [1] A. Leggett and A. Garg, Phys. Rev. Lett. **54**, 857 (1985).
 - [2] A. Leggett, Contemp. Phys. **25**, 583 (1984).
 - [3] A. Caldeira and A. Leggett, Ann. Phys. (N.Y.) **149**, 374 (1983).
 - [4] H. Grabert, P. Olschowski, and U. Weiss, Phys. Rev. B **36**, 1931 (1987).
 - [5] R.F. Voss and R.A. Webb, Phys. Rev. Lett. **47**, 265 (1981).
 - [6] S. Schwartz, B. Sen, C. Archie, and J. Lukens, Phys. Rev. Lett. **55**, 1547 (1985).
 - [7] J.M. Martinis, M.H. Devoret, and J. Clarke, Phys. Rev. B **35**, 4682 (1987).
 - [8] J.M. Martinis, M.H. Devoret, and J. Clarke, Phys. Rev. Lett. **55**, 1543 (1985).
 - [9] A. Larkin and Y.N. Ovchinnikov, Sov. Phys. JETP **64**, 185 (1986).
 - [10] P. Kopietz and S. Chakravarty, Phys. Rev. B **38**, 97 (1988).
 - [11] A. Leggett *et al.*, Rev. Mod. Phys. **59**, 1 (1987).
 - [12] U. Weiss, H. Grabert, and S. Linkwitz, J. Low Temp. Phys. **68**, 213 (1987).
 - [13] S. Han, J. Lapointe, and J. Lukens, Phys. Rev. Lett. **66**, 810 (1991).
 - [14] D.D. Awschalom, D.P. DiVincenzo, and J.F. Smyth, Science **258**, 414 (1994).
 - [15] A. Garg, Phys. Rev. Lett. **74**, 1458 (1995).
 - [16] A. Zhuravlev and A. Zorin, Sov. J. Low Temp. Phys. **16**, 102 (1990).
 - [17] J. Schmidt, A. Cleland, and J. Clarke, Phys. Rev. B **43**, 229 (1991).
 - [18] S. Han, J. Lapointe, and J. Lukens, in *Activated Barrier Crossing*, edited by G. Fleming and P. Hänggi (World Scientific, Singapore, 1993), 1st ed., Chap. 9, pp. 241–267.
 - [19] D. Esteve, M.H. Devoret, and J.M. Martinis, Phys. Rev. B **34**, 158 (1986).
 - [20] W. Bialek, S. Chakravarty, and S. Kivelson, Phys. Rev. B **35**, 120 (1987).